JOURNAL OF MATERIALS SCIENCE 28 (1993) 6753–6760

Reactivity of oxygen-deficient Mn(II)-bearing ferrites ($Mn_xFe_{3-x}O_{4-\delta}$, $0 \leqslant x \leqslant 1$, $\delta > 0$) toward CO_2 decomposition to carbon

MASAHIRO TABATA, KAZUHIRO AKANUMA, KEN'ICHI NISHIZAWA, KEISUKE MIMORI, TAKASHI YOSHIDA, MASAMICHI TSUJI, YUTAKA TAMAURA*
Department of Chemistry, Research Center for Carbon Recycling & Utilization, Tokyo Institute of Technology, Ookayama, Meguro-ku, Tokyo 152, Japan

The reduction of CO_2 to carbon was studied in oxygen-deficient Mn(II)-bearing ferrites ($Mn_xFe_{3-x}O_{4-\delta}$, $0 \leqslant x \leqslant 1$, $\delta > 0$) at 300 °C. They were prepared by reducing Mn(II)-bearing ferrites with H_2 gas at 300 °C. The oxygen-deficient Mn(II)-bearing ferrites showed a single phase with a spinel structure having an oxygen deficiency. The decomposition reaction of CO_2 to carbon was accompanied by oxidation of the oxygen-deficient Mn(II)-bearing ferrites. The decomposition rate slowed when the Mn(II) content in the Mn(II)-bearing ferrites increased. A Mössbauer study of the phase changes of the solid samples during the H_2 reduction and CO_2 decomposition indicated the following. Increases in the Mn(II) content lowered the electron conductivity of the Mn(II)-bearing ferrites. Increases in the oxygen deficiency, δ, contributed to an increase in electron conductivity and suggested that electron conduction due to the electron hopping determines the reductivity of CO_2 to carbon by the donation of an electron at adsorption sites.

1. Introduction

The reduction of CO_2 to CO and to hydrocarbons such as CH_4, CH_3OH or CHOOH by electrochemical, photochemical and catalytic reactions has been studied by many investigators [1–15]. In these electrochemical and photochemical reactions, the reactions are allowed to take place in an aqueous solution and CO_2 is reduced on the surface of the electrodes in the form of carbonate ions. The products are CO or hydrocarbons such as CH_3OH or CHOOH, and there have been no reports of carbon formation using these reactions [1–12]. Sacco and Reid [13] studied the decomposition of CO_2 with H_2 using metallic iron as a catalyst (Bosch reaction). They reported the deposition of carbon from CO_2 on the surface of the iron catalyst at 527–627 °C. Metallic iron has been known to decompose CO_2 gas to carbon in the presence of H_2 gas and the iron oxides were formed in the iron catalyst during the reaction with CO_2. They concluded that the metallic iron was oxidized by H_2O formed by the hydrogenation of CO_2 with H_2; this hydrogenation of CO_2 takes place concurrently with the catalytic reaction of the metallic iron, which produces H_2O. Lee *et al.* [14] found that the metallic iron was progressively transformed into a mixture of iron oxide (magnetite) and carbides during the course of the decomposition reaction of CO_2 gas by H_2. Thus, the CO_2 decomposition to carbon with metallic iron in the presence of H_2 gas was accompanied by side reactions such as the hydrogenation of CO_2 and the formation of carbides. The decomposition of CO_2 gas with metals in the absence of H_2 gas has been studied for some alkaline-earth metals such as calcium, strontium and barium [15]. These alkaline-earth metals can decompose CO_2 to carbon. These reports show that the CO_2 molecule is decomposed to carbon in a reaction in which oxygen from the CO_2 is incorporated into the metals to form each of the carbides. However, there have been no reports concerning the decomposition of CO_2 to carbon with metal oxides.

Recently, two of the present authors reported that an oxygen-deficient magnetite can break the chemical bond of CO_2 to form carbon with high efficiency (nearly 100%) at 300 °C [16]. In this reaction, the pressure of the CO_2 in the reaction cell is almost zero after completion of the reaction. This is due to the incorporation of oxygen from the CO_2 into the oxygen-deficient site of magnetite during the deposition of carbon. The high decomposition efficiency of CO_2 to carbon by oxygen-deficient magnetite is ascribed to the fact that the spinel structure of the magnetite is maintained during the reaction. More recently, a three-fragment adsorption mechanism was reported [17] in the study of the adsorption enthalpy and adsorption isotherm of CO_2 on oxygen-deficient magnetite in the temperature range 150–300 °C. The high reactivity of this compound in the decomposition of CO_2 to carbon is considered to be due to reactive sites

*Author to whom correspondence should be addressed.

0022–2461

where an electron is readily donated to the carbon of the adsorbed CO_2. The authors have concluded that electron hopping between Fe^{2+} and Fe^{3+} ions in the spinel structure of the magnetite facilitates the donation of an electron at their reactive sites.

The present paper studies the CO_2 decomposition reaction with oxygen-deficient Mn(II)-bearing ferrites ($Mn_xFe_{3-x}O_{4-\delta}$, $0 \leqslant x \leqslant 1$, $\delta > 0$) and discusses the reactivity toward CO_2 decomposition on the basis of a Mössbauer study.

2. Experimental procedure

2.1. Materials

All the chemicals used were of analytical grade, and distilled water was used for the preparation of the solution. $FeSO_4 \cdot 7H_2O$, $MnSO_4 \cdot (4 \sim 6)H_2O$ and NaOH were supplied by Wako Chemical Industries, Ltd.

2.2. Preparation of Mn(II)-bearing ferrites

Mn(II)-bearing ferrites were synthesized by air oxidation of aqueous suspensions of Fe(II) and Mn(II) mixed hydroxides [18]. Requisite quantities of $FeSO_4 \cdot 7H_2O$ and $MnSO_4 \cdot (4 \sim 6)H_2O$ were dissolved in O_2-free and CO_2-free distilled water (4 dm^3) by passing nitrogen gas through the water for a few hours. The pH of the solution was adjusted to 10 by adding 3 mol dm^{-3} of a NaOH solution to form a hydroxide suspension. Air was passed through the alkaline suspension for oxidation at 65 °C for 6 h. The reaction pH was kept constant at 10 by addition of the NaOH solution. The product was collected by decantation, then successively washed with distilled water and acetone, and then dried *in vacuo* at 65 °C.

The products were identified both by X-ray diffractometry (XRD) using FeK_α radiation (Rigaku model RAD-2A diffractometer) and Mössbauer spectroscopy. All the Mössbauer spectrometry (MS) was recorded at room temperature with a ^{57}Co (diffused in metallic Rh) source oscillated in a constant-acceleration mode. The spectra were calibrated with thin absorbers of an α-Fe foil. The products were analysed both by inductively coupled plasma (ICP) spectroscopy (Seiko Instruments Plasma Spectrometer model SPS 7000) for the Mn^{2+} and Fe_{total} contents and by colourimetry (Hitachi photospectrometer model 124) using 2,2′-bipyridine for the Fe^{2+} and Fe_{total} ratio [19].

2.3. Preparation of oxygen-deficient Mn(II)-bearing ferrites and their reactivity for CO_2 decomposition reaction

The experimental procedure and equipment were similar to those in a previous study [20] and are described only briefly. Mn(II)-bearing ferrite (1.00 g) was placed in a quartz cell (20 mm in diameter and 200 mm long). The cell was heated to 300 °C in an electric furnace while the reaction cell was evacuated using an oil rotary pump. After evacuating the reaction cell for 5 min at 300 °C, H_2 gas was allowed to pass through to reduce the Mn(II)-bearing ferrite in the reaction cell at a flow rate of 0.2 dm^3 min^{-1} for 2 h at 300 °C. After the H_2-reduction process, the reaction cell was evacuated to remove any remaining H_2 gas, and CO_2 gas (2×10^{-3} dm^3 or 8.32×10^{-5} mol) was introduced into the reaction cell using a microsyringe (recorded as the zero reaction time). The internal gas species were determined by gas chromatography with a Thermal Conductivity Detector (Shimadzu model GC-8A, using Porapak Q and a molecular sieve 13X as adsorbents). The solid samples were quenched after the reaction by quickly placing the reaction cell into a refrigerant of ice/NaCl. The carbon deposited on the samples was determined using an elemental analyser (Perkin-Elmer model 2400 CHN analyser). The solid samples before and after the H_2 reduction were identified by MS. The solid phase of the samples before and after the CO_2 decomposition reactions were identified by XRD with FeK_α radiation.

3. Results and discussion

3.1. Formation of Mn(II)-bearing ferrites

Only peaks corresponding to the cubic spinel structure appeared in the XRD patterns of the Mn(II)-bearing ferrite prepared by the air oxidation of the alkaline suspension. Chemical analysis showed that the Mn(II) content in the ferrite increased with increasing Mn(II) content of the initial solution. The chemical compositions and the lattice constants, a_0 of the Mn(II)-bearing ferrites are presented in Table I. The lattice constants increased linearly with the Mn(II) content, which is in accord with previously reported results [21]. The Mn(II)-bearing ferrites thus prepared were used in the following study of the CO_2 decomposition reaction.

3.2. Characterization of oxygen-deficient Mn(II)-bearing ferrites

The XRD patterns of the prepared H_2-reduced Mn(II)-bearing ferrites showed only peaks corresponding to the cubic spinel structure. No peaks corresponding to α-iron, metallic manganese, FeO, MnO or other iron and manganese compounds were observed, indicating that the sample consists of a single phase of the spinel structure. The δ-values and the lattice constants of the H_2-reduced Mn(II)-bearing ferrites are presented in Table II. The δ-values were calculated from the chemical-analysis data. The lattice constants of these compounds increased with reduction by H_2. This increase in the lattice constants is related to changes in the chemical compositions.

TABLE I The lattice constant and chemical composition of Mn(II)-bearing ferrites

Sample	r_{Mn}[a]	Chemical composition	Lattice constant (nm)
a	0	$Mn^{2+}_{0.00}Fe^{2+}_{0.81}Fe^{3+}_{2.19}O^{2-}_{4.09}$	0.8387
b	0.12	$Mn^{2+}_{0.32}Fe^{2+}_{0.34}Fe^{3+}_{2.34}O^{2-}_{4.17}$	0.8413
c	0.35	$Mn^{2+}_{0.78}Fe^{2+}_{0.21}Fe^{3+}_{2.01}O^{2-}_{4.00}$	0.8460
d	0.50	$Mn^{2+}_{1.00}Fe^{2+}_{0.00}Fe^{3+}_{2.00}O^{2-}_{4.00}$	0.8498

[a] Molar ratio of Mn/Fe in the samples.

TABLE II Lattice constant and oxygen deficiency, δ, in H_2-reduced Mn(II)-bearing ferrites ($Mn_xFe_{3-x}O_{4-\delta}$)

Sample	r_{Mn}[a]	Chemical composition[b]	δ	Lattice constant (nm)
a′	0.0	$Mn^{2+}_{0.00}Fe^{2+}_{1.14}Fe^{3+}_{1.86}O^{2-}_{3.93}$	0.07	0.8399
b′	0.1	$Mn^{2+}_{0.32}Fe^{2+}_{0.88}Fe^{3+}_{1.80}O^{2-}_{3.90}$	0.10	0.8433
c′	0.3	$Mn^{2+}_{0.78}Fe^{2+}_{0.52}Fe^{3+}_{1.70}O^{2-}_{3.85}$	0.15	0.8474
d′	0.5	$Mn^{2+}_{1.00}Fe^{2+}_{0.11}Fe^{3+}_{1.89}O^{2-}_{3.94}$	0.06	0.8501

[a] Molar ratio of Mn/Fe in the samples.
[b] Reduction time = 2 h.

TABLE III Mössbauer parameters of the oxygen-deficient magnetites obtained by 0, 1 and 2 h of H_2-reduction of magnetite at 300 °C

Sample	Reduction time (h)	Isomer shift[a] ($mm\,s^{-1}$)		A-to-B area ratio
		A	B	
a	0	0.29	0.66	0.85
	1	0.28	0.66	0.51
a′	2	0.27	0.66	0.54

[a] The isomer shifts are relative to the values for Fe.

These changes in the chemical compositions indicate that some of the Fe^{3+} ions in the Mn(II)-bearing ferrites are reduced. The increase in the lattice constant is closely related to the reduction of Fe^{3+} ions in the Mn(II)-bearing ferrites to Fe^{2+} ions. Thus, oxygen-deficient Mn(II)-bearing ferrites could be prepared which possessed a spinel structure.

The Mössbauer spectra were recorded for the H_2-reduced magnetites with the objective of obtaining information on the cation distribution (Fig. 1a, b and c). Only the absorption lines characteristic of the magnetite appeared in all the MS patterns of the reduced magnetites; two sextet absorption lines appeared. One sextet is the spectra corresponding to the Fe^{3+} ions in the A-sites, indicated by A, and the second sextet is the spectra corresponding to the Fe ions in the B-sites, indicated by B. No individual absorption peaks of Fe^{2+} and Fe^{3+} ions in the B-sites are seen because of the fast electron interchange at the B-sites (electron hopping) [22–25]. The Mössbauer parameters are presented in Table III. The area ratio of A-to-B sites should be 0.50×1.00 in stoichiometric magnetite (Fe_3O_4). The value 1.00 is the ratio of the recoil-free fractions determined by Weber and Hafner [26]. The chemical composition of the magnetite obtained in the present study is expressed as $Fe_3O_{4.09}$ which is a slightly oxidized (non-stoichiometric or cation-deficient) form of magnetite. It showed that there is a large A/B ratio of 0.85 in the MS parameter. This may be interpreted as follows. Voleník *et al.* [27] reported that in the MS of the stoichiometric and non-stoichiometric (cation-deficient) magnetites ($Fe_3O_{4-\delta}$, $\delta \leqslant 0$), the area ratio of the A-to-B sites increased as the cation deficiency increased. In stoichiometric magnetite, the number of Fe^{2+} ions is equal to the number of Fe^{3+} ions in the B-sites. These Fe^{3+} ions contribute to the B-site spectra. The oxidation of Fe^{2+} ions results in the formation of non-stoichiometric magnetite which contributes to the increase in the number of Fe^{3+} ions in the B-sites. Thus, the numbers of unpaired Fe^{3+} ions in the B-sites increase when the non-stoichiometry proceeds. These unpaired Fe^{3+} ions do not contribute to the B-site spectra but do contribute to the A-site spectra [27]. Thus, when the prepared magnetite is reduced to the stoichiometric composition, the A-to-B-site ratio should decrease to 0.50. When magnetite of stoichiometric composition was further reduced to form oxygen-deficient magnetite ($Fe_3O_{4-\delta}$, $\delta > 0$), the area ratio of A-to-B sites became larger than 0.5 (Fig. 1b and c, Table III). The increase in the area ratio is in accord with previous studies [28, 29]. This increase is considered to be due to the contribution of Fe^{2+} ions in the interstices of the A-sites which migrated from the B-sites [29].

The MS of typical H_2-reduced and unreduced Mn(II)-bearing ferrites with $r_{Mn} = 0.35$ are shown in Fig. 2. The lines of the B-sites are asymmetrically broadened compared to those of the magnetite shown in Fig. 1. These broadenings are principally caused by Mn^{2+} substitution in the A-sites and B-sites which produces different chemical environments from magnetite. They may be understood on the basis of the findings by Sawatzky *et al.* [30]. They studied the MS of Mn(II)-ferrites with $r_{Mn} = 0.5$ over a temperature range $298 \sim 475$ k with, and without an applied magnetic field, and they also observed the broadened spectra of B-sites. The authors fitted them into four sublines assuming that the intensities of the four Lorentzians forming the B-site line were constrained to be proportional to the probability that Fe ions in the B-sites have 3, 4, 5 or 6 nearest neighbour Mn(II) ions in the A-sites. The probabilities were calculated using the equation

$$I_n = \binom{6}{n}(1-c)^{6-n}c^n \qquad (1)$$

where I_n denotes the relative intensity of the B-site peak with $n Fe^{3+}$ ions in the nearest-neighbour A-sites, and c is the concentration of Fe^{3+} ions. For Mn(II)-bearing ferrite with $r_{Mn} = 0.50$, c is equal to 0.20 [31]. The fit is good and it indicates that the proposed model can reproduce the MS data.

As for Mn(II)-bearing ferrites with a lower Mn(II) content ($0 < r_{Mn} < 0.5$), the broadening has not clearly been interpreted. Therefore the authors tried to understand the broadening using the data of other metal-bearing ferrites. There have been some reports analysing the MS of magnetite doped with metallic ions in the B-sites or in the A-sites. Ok and Evans [32] reported the MS of Zn-bearing and Cd-bearing ferrites. The MS sextet pattern for the B-sites was broadened with an increase in the amount of Zn^{2+} or Cd^{2+}. The isomer shift of the peak which corresponds to the B-site in magnetite decreased with an increase in Zn or Cd content. Ok and Evans have pointed out that the ratio of the A-to-B-site area decreased with an increase in Zn or Cd content. However, the occupation of the A-sites with different cations left the Mössbauer

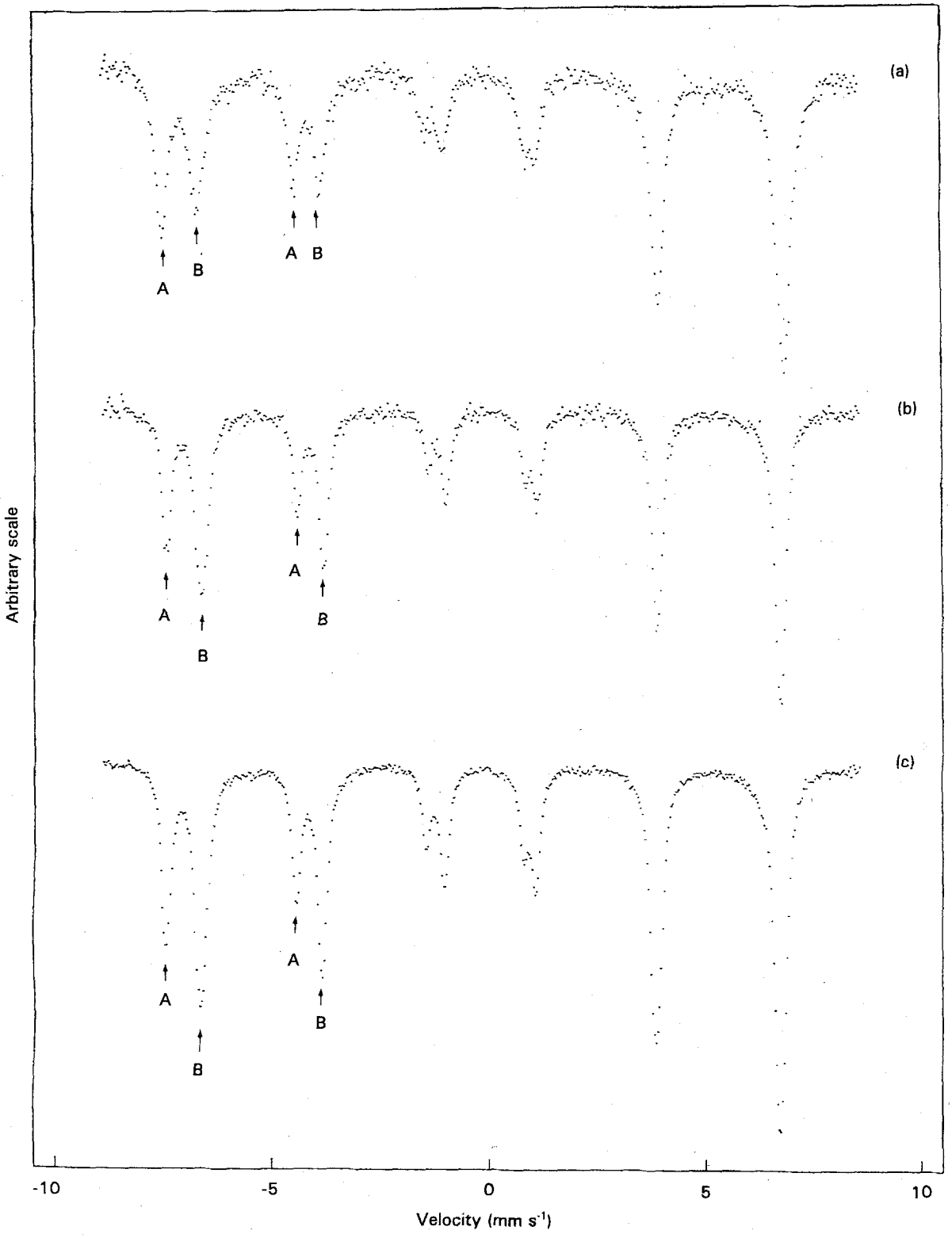

Figure 1 Mössbauer spectra of reduced magnetite for: (a) 0 h (sample a) (b) 1 h, and (c) 2 h (sample a')

parameters of the A-sites nearly unaffected. Franke and Rosenbery [33] reported on the MS of the Cr^{3+}-doped magnetites ($Cr_xFe_{3-x}O_4$ with $0 \leqslant x \leqslant 0.7$). Cr^{3+} ions are known to occupy only the B-sites. Franke and Rosenberg reported that the spectra assigned to the B-sites were broadened; this was also found in our MS of Mn(II)-bearing ferrites. Franke and Rosenberg dissolved the broadened spectra into the four most probable cation configurations in the B-sites as follows:

configuration (a) $3Fe^{3+} + 3Fe^{2+}$

configuration (b) $2Fe^{3+} + 3Fe^{2+} + 1Cr^{3+}$

configuration (c) $1Fe^{3+} + 3Fe^{2+} + 2Cr^{3+}$

configuration (d) $3Fe^{2+} + 3Cr^{3+}$

Thus, the B-site spectra are composed of four sextets. The sextet contributed by configuration (a) corresponds to the spectra of the B-site in stoichiometric magnetite, and the spectra of configuration (d) should

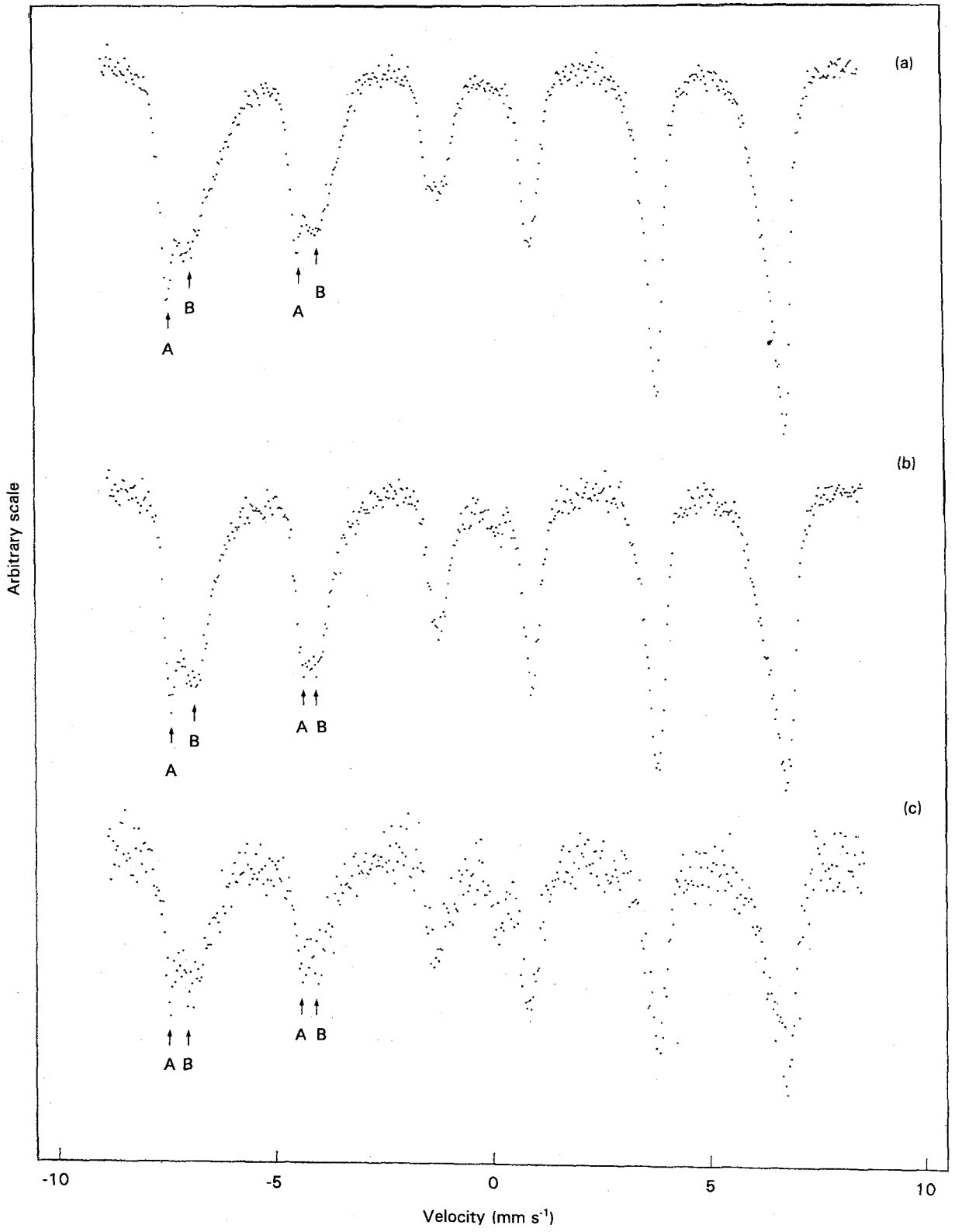

Figure 2 Mössbauer spectra of reduced Mn(II)-bearing ferrite with $r_{Mn} = 0.35$ for: (a) 0 h (sample c), (b) 1 h, and (c) 2 h (sample c').

contribute to a "pure" Fe^{2+} hyperfine field value in the B-site. These studies suggest that the doping of Mn(II) ions in both A- and B-sites caused the broadening of the MS of the B-sites.

Here the interpretation of the spectra of reduced Mn(II)-bearing ferrites is based on the above findings of metal-bearing ferrites. When the δ-value of Mn(II)-bearing ferrite increased, the peaks assigned to the B-sites were sharpened (Fig. 2b and c). The broadened peak became more symmetrical. Fe^{2+} ions are known to occupy the B-sites. Thus, the A-site is occupied by Mn^{2+} ions and a portion of Fe^{3+} ions and the B-site is occupied by Mn^{2+}, Fe^{2+} and Fe^{3+} ions. When Mn(II)-bearing ferrite is reduced, Fe^{3+} ions in both the A- and B-sites are reduced. In the case of the Fe^{3+} ions in the A-sites the Fe^{2+} ions formed cannot occupy the A-site and they migrate to the B-sites or to the surface of the solid. In the reduction of Fe^{3+} ions in the B-sites the Fe^{2+} ion formed can occupy the B-site and hence Fe^{3+} migration is not necessary. Thus, when Mn(II)-bearing ferrite is reduced, the reduction of Fe^{3+} ions in the B-sites is energetically easier than

that of Fe^{3+} ions in the A-sites. From this consideration, it can be assumed that Fe^{2+} ions increase only in the B-sites according to the level of the reduction. Thus, the sharpening of the B-site spectra can be explained by the increase in the number of Fe^{2+} ions in the B-sites in the oxygen-deficient Mn(II)-bearing ferrite. The Fe^{2+} ions form configuration (a) above and take part in fast electron hopping between Fe^{2+} and Fe^{3+} ions in the B-sites.

3.3. CO_2 decomposition reaction with oxygen-deficient Mn(II)-bearing ferrites

The decomposition of CO_2 was studied in oxygen-deficient Mn(II)-bearing ferrites at three levels of Mn(II) substitution, $r_{Mn} = 0.12$, 0.35 and 0.50. The result with $r_{Mn} = 0.12$ (sample b') at 300 °C is shown in Fig. 3. CO_2 was initially introduced at pressures up to 6.8×10^3 Pa in the reaction cell. The CO_2 content decreased gradually and was less than 25% after 4 h. On the other hand, the CO content increased up to 12% of the injected CO_2 within the first few minutes of the reaction, then it gradually decreased, and it became less than 7% of the initial CO_2 amount after 4 h. No other gases were observed during the reaction, indicating that the internal gases consisted mainly of CO_2 and CO. The lattice constant of the oxygen-deficient Mn(II)-bearing ferrite after the CO_2-decomposition reaction was restored to that of the unreduced Mn(II)-bearing ferrite. The content of carbon formed in the solid sample was 0.8744 mg per gram of sample, which was nearly equal to the value calculated from the amount of diminished CO_2 in the reaction cell. These results indicate that CO_2 is decomposed to carbon and that the oxygen in CO_2 is transferred into the crystal lattice in the form of O^{2-} ions to the oxygen-deficient Mn(II)-bearing ferrite.

Figs 4 and 5 show the time variations of the gas content during the reaction with oxygen-deficient Mn(II)-bearing ferrites with $r_{Mn} = 0.35$ (sample c') and 0.50 (sample d'), respectively. Similar patterns for CO_2 decrease and CO evolution can be seen in both samples. However, the amount of CO detected was small

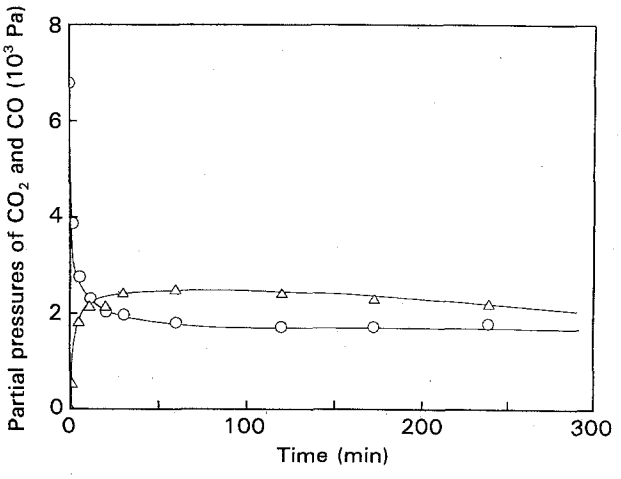

Figure 3 The change in the composition of (○) CO_2 and (△) CO during the CO_2-decomposition reaction with the oxygen-deficient Mn(II)-bearing ferrite (sample b') at 300 °C.

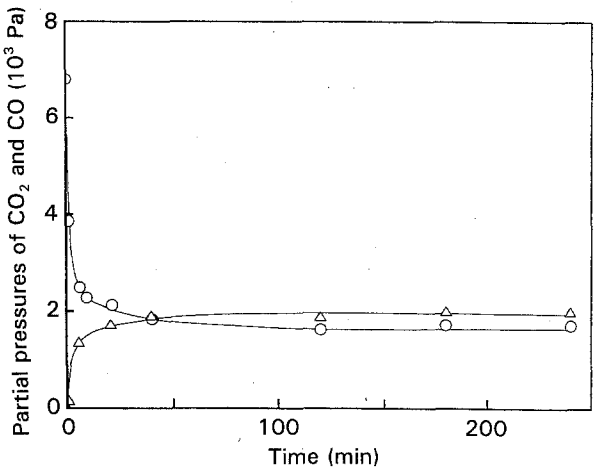

Figure 4 The change in the composition of (○) CO_2 and (△) CO during the CO_2-decomposition reaction with the oxygen-deficient Mn(II)-bearing ferrite (sample c') at 300 °C.

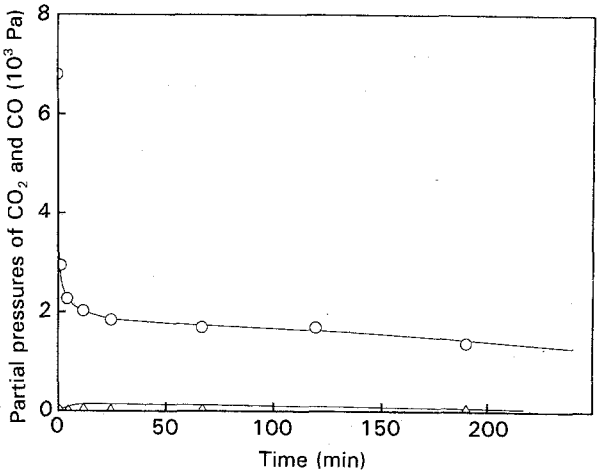

Figure 5 The change in the composition of (○) CO_2 and (△) CO during the CO_2-decomposition reaction with the oxygen-deficient Mn(II)-bearing ferrite (sample d') at 300 °C.

compared to the decrease in the amount of CO_2. The amount of carbon deposited was 0.48 mg per gram of sample for sample c' ($r_{Mn} = 0.35$) and 0.31 mg per gram of sample for sample d' ($r_{Mn} = 0.50$). There were no gases of carbon compounds except CO and CO_2. No peaks corresponding to carbides were observed in the XRD. The lattice constants of these oxygen-deficient Mn(II)-bearing ferrites after CO_2 decomposition were restored to the initial values of the Mn(II)-bearing ferrite.

Fig. 6 shows the relationship between the CO content after 1 h of reaction and r_{Mn}. The maximum CO content can be seen at $r_{Mn} = 0.12$. This relationship shows that the amount of Mn(II) ions in the oxygen-deficient Mn(II)-bearing ferrite will regulate the decomposition reaction of CO_2 to CO. In the sample b', the decrease in the amount of CO_2 and the amount of CO evolved are nearly equal. The existence of Mn(II) ions interfered with the decomposition of CO_2 to carbon and enhanced the evolution of CO instead. As r_{Mn} increased further, the amount of CO evolution decreased. Therefore, regulation of the r_{Mn}-value will enable oxygen-deficient Mn(II)-bearing ferrites to optimize the CO-evolution reaction instead of carbon

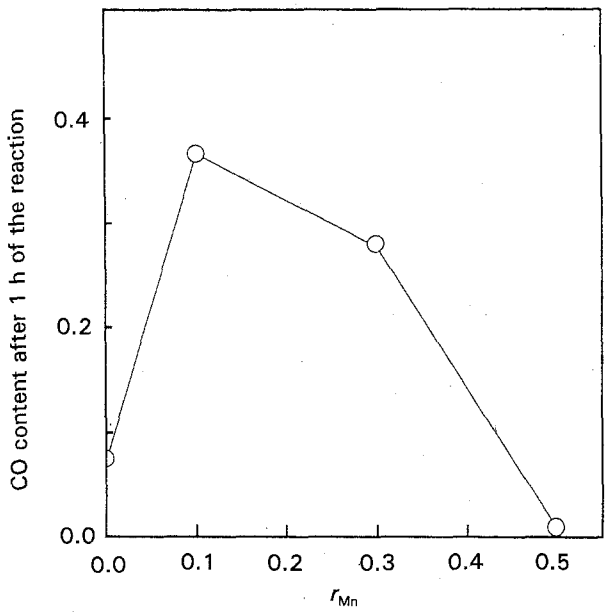

Figure 6 Relationship between CO content after 1 h of the CO_2-decomposition reaction and r_{Mn}.

deposition. The deposited amount of carbon is large compared to the evolved amount of CO in the oxygen-deficient Mn(II)-ferrite with a higher r_{Mn} value. CO_2 is non-specifically adsorbed on the Mn(II)-bearing ferrite; an increase in r_{Mn} leads to an increase in the non-specific adsorption of CO_2.

Table IV summarizes the relationship between the amount of deposited carbon and the r_{Mn}-value. The amount of carbon deposited decreased in comparison with that of sample b'. This is due to an increase in the portion of the adsorption of CO_2 and/or CO on the solids. The amounts of carbon are small compared to those calculated from the gas content. An increase in r_{Mn} results in a lowering of the amount of carbon deposited in milligrams per gram of sample. The amount was recalculated in mg g^{-1} per δ (Table IV). Since the δ-value in the oxygen-deficient Mn(II)-bearing ferrites is nearly constant, the difference in the amount of carbon deposited is ascribed to the effect of the Mn(II) content in the oxygen-deficient Mn(II)-bearing ferrite.

3.4. Relationship between electron hopping and CO_2-decomposition reactivity.

The reactivity of CO_2 decomposition to carbon of the oxygen-deficient Mn(II)-bearing ferrites tends to be low when r_{Mn} is large and the δ-value is small. In the MS data for the oxygen-deficient Mn(II)-bearing ferrites, broadening of the peaks assigned to the B-sites was observed when the r_{Mn}-value increased. When the Mn(II)-bearing ferrites are reduced by H_2 gas, the peaks were sharpened. This sharpening of the peaks implies there is an increase in the strength of the subpeaks assigned to $Fe^{2.5+}$; that is, the probability of electron hopping increases. The enhancement of electron hopping will facilitate the donation of electrons to the surface of the solid, and then to CO_2 adsorbed on the surface. Molecules of CO_2 adsorbed on the crystal face accept electrons to be reduced to

TABLE IV Relationship between the amount of deposited carbon and the r_{Mn}-value

Sample	r_{Mn}	Deposited carbon (mg per gram of sample)	δ	Deposited carbon (mg per gram of sample)δ^{-1}
a'	0	1.29	0.07	18
b'	0.12	0.874	0.10	8.7
c'	0.35	0.481	0.15	3.2
d'	0.50	0.313	0.06	6.3

$CO_{(adsorbed)}$ and $oxygen_{(adsorbed)}$. The donation of an electron results in the oxidation of Fe^{2+} ions to Fe^{3+} ions in the B sites of the spinel structure. Thus, the reactivity of the CO_2 decomposition of the oxygen-deficient Mn(II)-bearing ferrites can be understood on the basis of the probability of electron hopping.

4. Conclusion

Oxygen-deficient Mn(II)-bearing ferrite (r_{Mn} = 0, 0.12, 0.35 and 0.50) of a single phase with a spinel structure were obtained by reducing Mn(II)-bearing ferrites with H_2 gas at 300 °C for 1 ~ 2 h. Their lattice constants were larger than those of the unreduced forms. CO_2 has been found to be decomposed to carbon by the oxygen-deficient Mn(II)-bearing ferrite; this was accompanied by an evolution of CO. The amount of deposited carbon decreased with an increase in r_{Mn}, while the amount of CO increased. The amount of CO evolved drastically decreased when r_{Mn} = 0.50. The Mössbauer study showed that the probability of electron hopping between the B-sites increased as the reduction of the Mn(II)-bearing ferrite proceeded. An increase in the r_{Mn}-value contributed to the decrease in the probability of electron hopping. Mn^{2+} ions can occupy both the A- and B-sites of the spinel structure. The occupation of Mn^{2+} ions in the B-sites disturbs electron hopping between the B-sites. The rate of CO_2 decomposition to carbon decreased in oxygen-deficient Mn(II)-bearing ferrites with increases in the r_{Mn}-values, although the δ-value was larger than that of oxygen-deficient magnetite. These results indicate that the rate of CO_2 decomposition depends on the extent of electron hopping between the B-sites.

References

1. J. C. HEMMINGER, R. CARR and G. A. SOMORJAI, *Chem. Phys. Lett.* **57** (1978) 100.
2. T. INOUE, A. FUJISHIMA, S. KONISHI and K. HONDA, *Nature (London)* **277** (1979) 637.
3. K. OTSUKA, *Hyomen* **23** (1985) 206.
4. Y. HORI, A. MURATA and R. TAKAHASHI, *J. Chem. Soc. Faraday Trans. I* **85** (1989) 2309.
5. J. HAWECKER, J.-M. LEHN and R. ZIESSEL, *Helv. Chem. Acta* **69** (1986) 1990.
6. B. A. PARKINSON and P. F. WEAVER, *Nature (London)* **309** (1984) 148.
7. R. ZIESSEL, J. HAWECKER and J.-M. LEHN, *Helv. Chim. Acta.* **69** (1986) 1065.
8. S. IKEDA, T. TAKAGI and K. ITO, *Bull. Chem. Soc. Jpn.* **60** (1987) 2517.
9. J. A. MARCOS, R. H. BUITRAGO and E. A. LOMBARDO, *J. Catal.* **105** (1987) 95.

10. M. A. ULLA, R. A. MIGONE, J. O. PETUNCHI and E. A. LOMBARDO, *ibid.* **105** (1987) 107.
11. I. WILLNER and D. MANDLER, *J. Amer. Chem. Soc.* **111** (1989) 1330.
12. M. GRÄTZEL, A. J. McEVOY, K. R. TAMPI and C. REVILLIOD, in Proceedings of the International Symposium on the Chemical Fixation of Carbon Dioxide, Nagoya, 1991, edited by K. Ito (The Chemical Society of Japan, Nagoya, 1991) A1, pp. 1–10.
13. A. SACCO Jr and R. C. REID, *Carbon* **17** (1979) 459.
14. M.-D, LEE, J.-F.LEE and C.-S. CHANG, *J. Chem. Engng. Jpn.* **23** (1990) 130.
15. "Gmelins handbuch der anorganischen chemie", 8th Edn, Kohlenstoff Part C2 (Springer Verlag, Berlin, 1972) pp. 203.
16. Y. TAMAURA and M. TABATA, *Nature (London)* **346** (1990) 255.
17. K. NISHIZAWA, T. KODAMA, M. TABATA, T. YOSHIDA, M. TSUJI and Y. TAMAURA *J. Chem. Soc. Faraday Trans.* **88** (1992) 2771.
18. M. KIYAMA, *Bull. Chem. Soc. Jpn.* **51** (1978) 134.
19. I. IWASAKI, T. KATSURA, T. OZAWA, M. YOSHIDA, M. MASHIMA, H. HARAMURA and B. IWASAKI, *Bull. Volcanol. Soc. Jpn. Ser II.* **5** (1960) 9.
20. M. TABATA, Y. NISHIDA, T. KODAMA, K. MIMORI, T. YOSHIDA and Y. TAMAURA, *J. Mater. Sci.* **28** (1993) 971.
21. Z. FUNATOGAWA, N. MIYATA and S. USAMI, *J. Phys. Soc. Jpn.* **14** (1959) 1583.
22. E. J. W. VERWEY and P. W. HAAYMAN, *Physica* **8** (1941) 979.
23. D. S. TANNHAUSER, *J. Phys. Chem. Solids* **23** (1962) 25.
24. A. ROSCENCWAIG, *Can. J. Phys.* **47** (1969) 2309.
25. W. KÜNDIG and R. HORGROVE, *Solid State Commun.* **7** (1969) 223.
26. H.-P. WEBER and S. S. HAFNER, *Z. Kristallogra.* **133** (1971) 327.
27. K. VOLENÍK, M. SEBERÍNI and J. NEID, *Czech. J. Phys. B* **25** (1975) 1063.
28. T. YOSHIDA, K. NISHIZAWA, M. TABATA, H. ABE, T. KODAMA, M. TSUJI and Y. TAMAURA, *J. Mater. Sci.* **28** (1993) 1220.
29. Y. TAMAURA, in Proceedings of International Symposium on Chemical Fixation of Carbon Dioxide, Nagoya, 1991, edited by K. Ito. (The Chemical Society of Japan, Nagoya, 1991) B5, pp. 167–172.
30. G. A. SAWATZKY, F. V. D. WOUDE and A. H. MORRISH, *Phys. Rev.* **187** (1969) 747.
31. J. H. HASTINGS and L. M. CORLISS, *ibid.* **104** (1956) 328.
32. H. N. OK and B. J. EVANS, *Phys. Rev. B* **14** (1976) 2956.
33. H. FRANKE and M. ROSENBERG, *J. Magnet. Mag. Mater.* **9** (1979) 74.

Received 5 February
and accepted 24 May 1993